Polymer 51 (2010) 540–546

Contents lists available at ScienceDirect

Polymer

journal homepage: www.elsevier.com/locate/polymer

The effect of confinement in nanoporous polymers on the glass transition temperature

Tong Liu, Richard W. Siegel, Rahmi Ozisik*

Department of Materials Science and Engineering, and Rensselaer Nanotechnology Center, Rensselaer Polytechnic Institute, MRC-205, Troy, NY 12180, USA

ARTICLE INFO

Article history:
Received 18 September 2009
Received in revised form
27 October 2009
Accepted 13 November 2009
Available online 4 December 2009

Keywords:
Glass transition
Confinement
Nanopores

ABSTRACT

The glass transition temperature (T_g) of nanoporous polyetherimide (PEI) and PEI thin films was investigated. The T_g decreased from its bulk value in both of these confined systems. Monte Carlo simulations were performed to calculate the nearest neighbor pore-to-pore distances in the nanoporous PEI. A quantitative analogy between the nanoporous PEI and PEI thin films is proposed through an equivalence of nearest neighbor pore-to-pore distances and thin film thickness. The effect of confinement is believed to be due to the interface regions, which possess higher chain mobility than the bulk. When these high mobility interface regions are sufficiently close together, the excess mobility at the interface region affects the dynamics of the system by restraining percolation of the slow domains resulting in the observed decrease in T_g.

1. Introduction

The glass transition temperature (T_g) is one of the most important properties of polymers because it indicates the dynamics of polymer chains and controls many practical processes such as welding, adhesion, and melt-processing [1]. Additionally, around the glass transition temperature, the mechanical properties of polymers change rapidly from a rubbery to a glassy state. Research on glass transition behavior in polymers has been an active subject for a long time, however, our understanding of the underlying science of the glass transition is still not fully complete.

The glass transition phenomenon received close attention over the past ten years as new techniques were developed to probe the intrinsic length scale of cooperative rearranging regions (CRRs). The so-called CRR was proposed by Adam and Gibbs [2], and is defined as the smallest region that can undergo a transition to a new configuration independent of neighboring regions [2]. The CRRs are domains of several nanometers in size [3]. This proposal led to a huge interest in the investigation of the glass transition temperature in polymers under confined geometries. A number of experimental studies have concentrated on various confined systems. For example, one approach was to use nanoporous glass with controlled pore size as host and to fill the pores with polymers by capillary wetting. As a result, reduced T_g values and enhanced chain dynamics have been reported [4]. However, a complication of this approach is that the internal glass surface could itself strongly affect the chain dynamics beyond the effects of confinement [5].

An attractive alternative system is polymer thin films, in which the confining dimension is the film thickness. Since the initial measurement of T_g in polystyrene (PS) thin films supported by a silicon substrate performed by Keddie et al. [6], both substrate-supported and unsupported (free-standing) thin films of different polymers have been studied. Deviations of glass transition temperature from the bulk T_g value have been reported when the film thickness decreased below ~150 nm. It was observed that the T_g values depend strongly on the interface between the polymer film and the substrate [7–9]. When the interaction between the film and the substrate is weak, the T_g of the film has a lower value than the corresponding bulk value. The T_g of the film is greater than the bulk value when there exists a strong interface between the film and the substrate because of the strong adhesion of polymer chains to the substrate. The influence of the polymer-substrate interaction can be eliminated in free-standing polymer thin films, where only a reduction in T_g is observed [5,10]. In addition to the dependence on the polymer-substrate interface, further studies on the glass transition behavior in polymer thin films showed a complex molecular weight dependence [5,10,11]. At high molecular weights, the T_g increases linearly with film thickness. At low molecular weights, the change in T_g shows a nonlinear film thickness dependence.

In order to interpret the phenomenon observed in polymer thin films and understand the glass transition behavior, many

* Corresponding author.
E-mail address: ozisik@rpi.edu (R. Ozisik).

0032-3861/$ – see front matter © 2009 Elsevier Ltd. All rights reserved.
doi:10.1016/j.polymer.2009.11.026

attempts have been made to generate a quantitative connection between the intrinsic length scale of the cooperative rearranging regions and the length scale at which the confinement effects on glass transition temperature are observed [6–8,11]. However, further research on the glass transition behavior in polymer thin films does not support this approach, since the size of the CRR near T_g was found to be in the range of 1–4 nm, while the length scale of the observed confinement effects on T_g is much larger [12]. More recently, with the development of new analysis techniques, such as positron annihilation lifetime spectroscopy (PALS) and scanning force microscopy (SFM), it has been observed that a significant depression of T_g near the thin film surface occurs as deep as several tens of nanometers, up to 100 nm, into the bulk region of the surface [12–15]. Enhanced polymer chain mobility near a free surface has been reported by many researchers, which is suggested to be mainly due to the segregation of chain ends at the free surface [16–18]. It is crucial to elucidate the mechanisms for the excess chain mobility at the surface and to understand how this excess mobility can propagate further into the bulk region of the film. De Gennes [19,20] proposed a tentative model to explain the glass transition behavior in polymeric thin films at high molecular weights. In this model, the enhanced mobility of polymer chains at the free surface can propagate into the bulk of the film by a sliding motion, which is highly ineffective in the bulk, but plays a more important role in thin films. Long and Lequeux [21] proposed their model from a percolation viewpoint. They suggested that the domains of slow dynamics percolate at a lower temperature in a quasi-two-dimensional case of free-standing thin films compared to a three-dimensional bulk glass transition.

Polymer nanocomposites have attracted a lot of interest due to the many unusual combinations of properties they offer. Because of their large filler/polymer interfacial area, research on the glass transition behavior in polymer nanocomposites has caught a lot of attention recently. Similar to the observations in polymer thin films, deviations of glass transition temperature from the bulk value have been reported in different polymer nanocomposite systems [22–27]. Both the sign and the magnitude of the shift in T_g values were found to be influenced by the interaction between the filler and the polymer matrix [24–27]. However, attempts to explain the glass transition behavior in polymer nanocomposites have been very limited from the theoretical viewpoint. Ash et al. [3,24] suggested an explanation by defining an interaction zone surrounding the nanofillers, which has different attributes compared to the bulk polymer. The impact of the interaction zone may extend tens to hundreds of nanometers into the bulk surrounding the nanofillers. Based on the percolation mechanisms, Ash et al. proposed that the region surrounding each nanofiller in a non-wetting filler/polymer interface exists as a highly mobile interaction zone in the nanocomposite. When the temperature of the system increases, the percolation of the slow domains would be interrupted at lower temperatures because of the existence of these dispersed high mobility regions. This leads to a decreased glass transition temperature. Further insight was proposed by Bansal et al. [25,26], who compared the glass transition temperatures of both polymer thin films and polymer nanocomposites. Bansal et al. suggested a quantitative equivalence of the T_gs in both systems by using a harmonic average of the interparticle spacing. They also concluded that the glass transition process requires the interaction of the high mobility interface regions. Even though there have been many experimental and theoretical studies on the effects of confinement on the glass transition, our understanding of this issue is far from complete.

In this paper, we studied the glass transition behavior of nanoporous polyetherimide (PEI) and compared it with non-porous PEI thin films. The nanoporous PEI films were created based on the phase separation of PEI and polycaprolactone-diol (PCLD) blends and subsequent removal of the PCLD domains by selective solvent extraction. Chemical structures of PEI and PCLD are shown in Fig. 1. Scanning electron microscopy (SEM) and statistical methods were used to characterize the pore structure and to obtain the pore structure parameters. Nanoporous PEI films with different pore volume fractions were obtained by varying the initial PCLD content in the PEI/PCLD blends. The nearest neighbor pore-to-pore distances were calculated by Monte Carlo simulations based on the pore size distribution functions obtained from SEM experimental data. The T_g of the nanoporous PEI films was measured and compared to the T_g of the pure PEI thin films.

2. Experimental and simulation details

2.1. Materials

PEI (Ultem® 1000) with a weight average molecular weight (M_w) of 30,000 g/mol and number average molecular weight (M_n) of 12,000 g/mol was obtained from General Electric Plastics, Inc. The density of PEI is 1.28 g/cm^3. PCLD with M_n of 503 g/mol was purchased from Aldrich Corporation. The density of PCLD is 1.073 g/cm^3. Dichloromethane (boiling temperature = 40 °C) was used to dissolve both PEI and PCLD. Acetone was used to selectively remove PCLD from the PEI/PCDL blends.

2.2. Preparation of nanoporous PEI films

The preparation method of the nanoporous PEI samples was introduced in detail in our previous paper [27] and a brief summary is given here. PEI and PCLD were dissolved in dichloromethane and mixed by magnetic stirrer at room temperature. PEI/PCLD blend films were obtained by spin-coating at a speed of 500 rpm on highly polished silicon wafer substrates. The spin-coated PEI/PCLD film samples were immersed in acetone for over 48 hours to remove the PCLD and to create the nanoporous structure within the PEI matrix. The nanoporous PEI film samples were then dried at 40 °C in a vacuum oven for 48 hours. Thermal gravimetric analysis (TGA) measurements were performed to verify that the minor component (PCLD) was removed after acetone immersion.

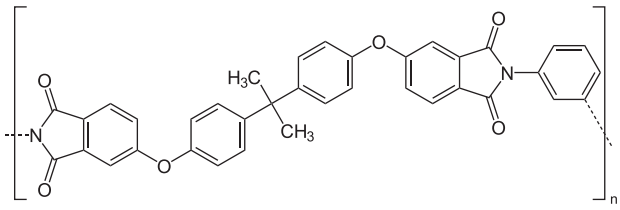

a

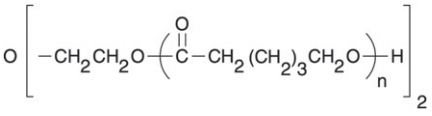

b

Fig. 1. Chemical structures of (a) polyetherimide, PEI and (b) polycaprolactam-diol, PCLD.

2.3. Pore structure characterization

A JEOL JSM-6330F field emission scanning electron microscope (FESEM) was used to observe the pore structure in the nanoporous PEI films. The cross-sections of the spin-coated films were prepared by microtoming and then the sample surfaces were sputter-coated with gold or platinum before SEM observation. SEM images were analyzed to quantitatively determine the pore size and pore size distribution. Statistical methods were applied to analyze the pore size data. The probability plot correlation coefficient (PPCC) hypothesis testing method was used to obtain the pore size distribution function and to estimate the distribution parameters [28,29].

2.4. The glass transition temperature measurement

The glass transition temperatures of the PEI thin films and the nanoporous PEI were measured by differential scanning calorimetry (DSC) on a Mettler Toledo DSC 822e instrument. All measurements were carried out from 25 to 250 °C at a heating rate of 10 °C/min in a nitrogen-filled chamber. The T_g data were established by fitting straight lines to the DSC curves before, during and after the transition. The midpoint of the intersections was then defined as the T_g. The DSC specimens were free-standing films that were obtained by removing the films from the substrate using a water bath. All film samples were dried in a vacuum oven at about 40 °C for 48 hours before DSC measurements.

2.4.1. Monte carlo simulation

Monte Carlo simulations were used to create three-dimensional periodic boxes containing nanopores. Only spherical pores were considered. Initially, no overlap between pores was allowed, however, the effect of pore overlap was also considered and investigated. The center of mass coordinates of each pore were created randomly. Pore sizes were assigned according to the (pore size) distribution function that was obtained from the pore structure characterization discussed above. We converted the probability distribution functions (PDFs) into cumulative distribution functions (CDFs), which by definition have values between zero and one, and used these CDFs in our Monte Carlo simulations. If the newly created pore did not overlap with any other existing pores, it was accepted and its coordinates were saved. If the randomly created pore overlapped with any previously crated pore then it was deleted. Each simulation was terminated once the target pore volume fraction, which was dictated by the PCLD content in the blend and pore structure analysis, was reached. The nearest neighbor pore-to-pore distances (surface-to-surface distances) were calculated from the saved coordinates of each pore within a system [30]. The results were averaged among ten or more simulations for each pore volume fraction.

3. Results

3.1. Characterization of pore structure

In the current study, the pores were created as a result of the phase separation of the immiscible polymer blends of PEI and PCLD. Therefore, pore size is directly related to the size of the phase-separated minor phase domains. There are many factors that would influence the size of the minor phase domains and the resultant pore size, such as polymer blend composition and molecular weight of the blend components and processing conditions [31–33]. In our previous paper [27], it was found that the processing time of phase separation played an important role in determining the final pore size due to the kinetics of the phase coarsening. Nano-size pores were created because of the fast film solidification during the spin-coating process. In addition, increasing the PCLD content resulted in larger pores due to the greater possibility for the minor phase domains to coalesce during phase coarsening.

The pore structure of the nanoporous PEI was investigated using SEM (27), and statistical methods were used to interpret the pore size data. Analysis of SEM micrographs and probability plot correlation coefficient (PPCC) hypothesis testing revealed that the pore size distribution is best represented by the lognormal distribution function:

$$f(x) = \frac{1}{x\sigma\sqrt{2\pi}}\exp\left\{-\frac{[ln(x/m)]^2}{2\sigma^2}\right\} \quad (1)$$

where σ is the shape parameter, and m is the median value of the data (also called the scale parameter), which is defined as:

$$\mathrm{m} = \exp(\bar{\mu}) \quad \text{and} \quad \bar{\mu} = \frac{\sum_i ln(x_i)}{N} \quad (2)$$

where x_i is the size of each observed pore and N is the total number of pores observed.

The shape and scale parameters of the lognormal probability density function (Eq. (1)) can be estimated by the PPCC method. Table 1 shows the shape and scale parameters of the probability density functions for nanoporous PEI samples with different initial minor phase contents. These parameters are useful to determine the probability density function that is required to perform the Monte Carlo simulations in order to obtain nearest neighbor pore-to-pore distances.

3.2. The nearest neighbor pore-to-pore distance

Monte Carlo simulation provides an efficient method to sample a statistical distribution [30,34]. We created three-dimensional nanoporous samples by performing Monte Carlo simulations. The simulations used the lognormal distribution functions obtained from the SEM analysis and, therefore, the simulated pore size distribution strictly followed the lognormal distribution function that represents the experimental data. The pore volume fraction (φ) was calculated from the PCLD weight content in the PEI/PCLD blend as:

$$\phi = \frac{w_{PCLD}/\rho_{PCLD}}{(w_{PCLD}/\rho_{PCLD}) + [(1 - w_{PCLD})/\rho_{PEI}]} \quad (3)$$

where w_{PCLD} is the PCLD weight content in the PEI/PCLD blend, ρ_{PCLD} and ρ_{PEI} are the density of PCLD and PEI, respectively. Based on Eq. (3), the pore volume fractions were 3.56, 5.91, 9.4, 11.7, 15.1, 17.4% and 23.0%.

Fig. 2 shows the comparison of the lognormal pore size distribution functions and the pore size distributions obtained from the Monte Carlo simulations. It is clearly seen that the two distributions agree perfectly. The pore structures obtained from the Monte Carlo simulations were used to calculate the distances between all pores.

Table 1
Lognormal distribution function parameters.

PCLD Content (wt%)	σ	m(nm)
3	0.535	50.2
5	0.449	54.2
8	0.314	56.3
10	0.392	59.1
13	0.369	60.3
15	0.375	69.0
20	0.360	75.3

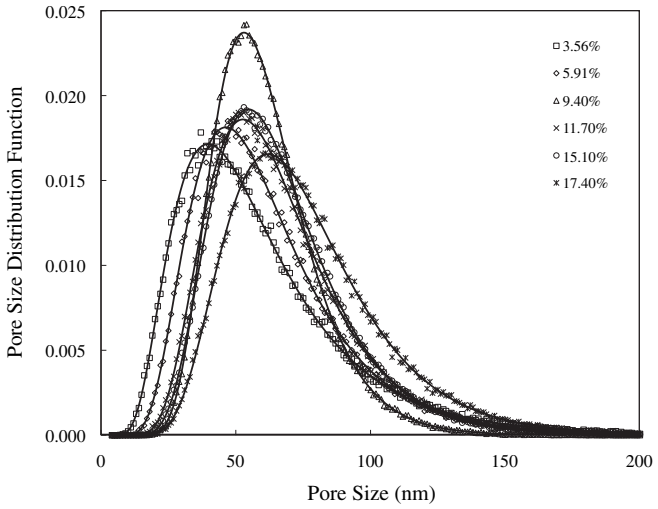

Fig. 2. The pore size distributions obtained from the Monte Carlo simulations (symbols) perfectly agree with the lognormal distribution functions (lines).

The nearest neighbor pore-to-pore (surface-to-surface) distances (d_{ij}) were calculated for each pore pair (*i* and *j*), and each pore pair was tabulated only once (d_{ji} values were removed).

Fig. 3 shows the nearest neighbor pore-to-pore distance probability distribution functions for pore volume fractions of 3.56, 5.91, 9.40, 11.7, 15.10, and 17.4%. Fig. 4 shows the arithmetic averages of the nearest neighbor pore-to-pore distances ($\bar{h}$) normalized by the average pore size ($\bar{r}$) as a function of pore volume fraction. The average pore-to-pore distance decreased with increasing pore volume fraction. The normalized pore-to-pore distances shown in Fig. 4 are lower than the close-packed sphere calculations, which show a $1.809\varphi^{-1/3}$-2.0 relationship with the pore volume fraction. If a similar relationship is assumed for the randomly created pores (with polydisperse size distribution), then $0.663\varphi^{-1/3}$-1.025 is obtained (dashed lines on Fig. 4).

3.3. The glass transition temperature

The glass transition temperatures of nanoporous PEI samples with varying pore volume fractions and PEI thin films were reported in our previous publication [27]. The T_g of nanoporous

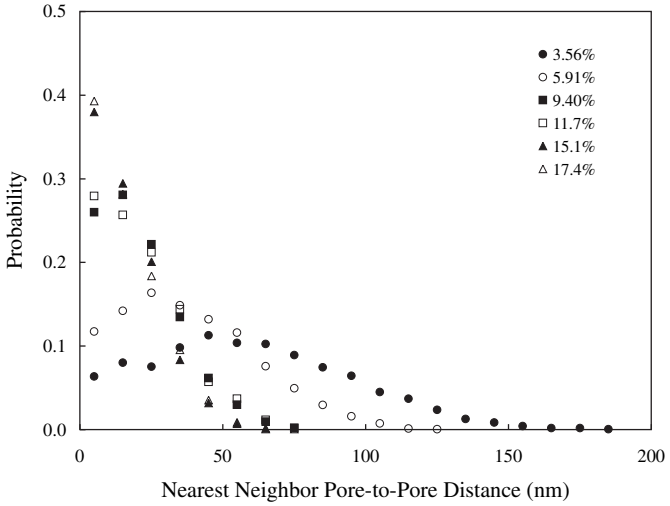

Fig. 3. Nearest neighbor pore-to-pore (surface-to-surface) distance distributions at various pore volume fractions.

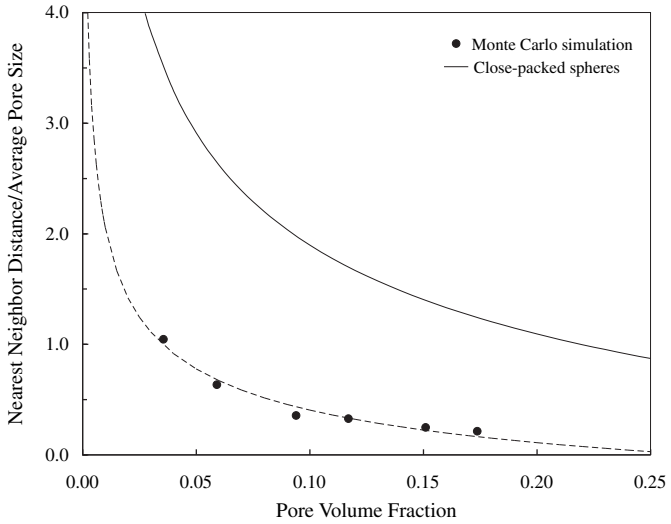

Fig. 4. Arithmetic average of the nearest neighbor pore-to-pore (surface-to-surface) distances normalized by the average pore size diameter as a function of pore volume fraction.

samples decreased ~22 K over the range of pore volume fractions from 0 to 0.23. Fig. 5 shows the glass transition temperatures of PEI thin films as a function of film thickness. The effect of decreasing film thickness and increasing pore volume fraction on the glass transition temperature was similar in that the glass transition temperature decreased in both cases. The T_g decreased by ~22 K in the nanoporous PEI and by −7 K in the thin films.

4. Discussion

The glass transition temperature of both PEI thin films and nanoporous PEI decreased with respectively decreasing film thickness and increasing pore volume fraction. It has been suggested that the existence of a high mobility interface region contributes to the T_g reduction. However, our present understanding of the properties of this high mobility interface region and the effects of this interface region on T_g are limited. Different approaches have been proposed to explain the thickness dependence of T_g in polymer thin films. The empirical model proposed by

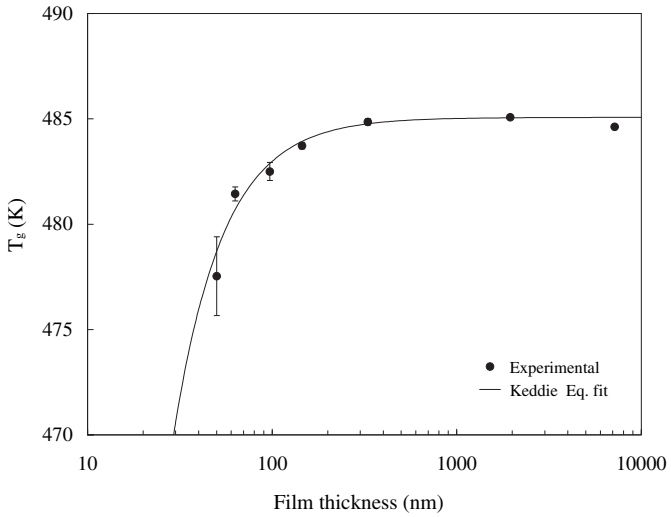

Fig. 5. Glass transition temperature of PEI thin films as a function of film thickness.

Keddie et al. [6,7] has been found to quantitatively interpret the experimental T_g data in polymer thin films quite well. According to Keddie et al. the relationship between T_g and the film thickness can be described by the following equation:

$$T_g(h) = T_g(\infty)\left[1 - \left(\frac{A}{h}\right)^{\delta}\right], \tag{4}$$

where h is the film thickness, $T_g(\infty)$ is the bulk glass transition temperature, and A and δ are fitting parameters. In the present study, the parameters A and δ were calculated using the PEI thin film data to be 3.38 nm and 1.61, respectively. Mattsson et al. [5] reported A and δ values for free-standing polystyrene thin films to be 7.8 nm and 1.8, respectively. The parameters obtained from our PEI thin films are very close to those obtained by Mattsson et al. The differences are attributed to the different chemical structures between polystyrene and PEI.

A direct comparison of the thin film and nanoporous T_g data can be made by transforming Keddie's equation so that it depends on specific surface area instead of thickness (see Eq. (5)). This transformation assumes that a two-layer model is applicable and, therefore, the comparison can also serve as a test of the two-layer model.

$$T_g(h) = T_g(\infty)\left[1 - \left(\frac{A}{2}\sigma\right)^{\delta}\right], \tag{5}$$

where σ is the specific surface area (surface area per volume, where volume is the product of surface area and film thickness, h). The factor two in the denominator is due to the presence of two free surfaces in a film. Fig. 6 shows the nanoporous T_g data (symbols) and modified Keddie equation, where parameters A and δ are those of our PEI thin films ($A = 3.38$ nm, $\delta = 1.61$). It is obvious that the modified Keddie equation with thin film parameters does not represent the nanoporous PEI T_g data. This suggests that the two-layer model cannot be used to explain the T_g data in nanoporous systems. In their recent study, Bansal et al. [26] reported a quantitative equivalence of T_gs between polymer thin films and polymer nanocomposites based on the two-layer model proposed by Mattsson [5]. They also concluded that a simple two-layer model is not sufficient to represent the effects of the interface region on T_g.

Although Keddie's equation has been used to represent experimental data successfully, it is an empirical model and does not explain the possible mechanisms of confinement effects on T_g.

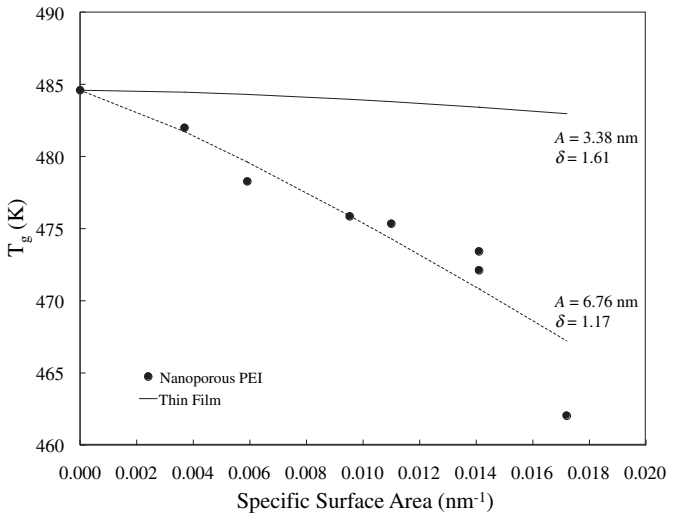

Fig. 6. Comparison of thin film and nanoporous T_g data as a function of specific pore surface area.

More recently, a very similar equation was proposed by Long and Lequeux based on the percolation theory of glass transition [21] and provides a theoretical explanation for Keddie's equation through heterogeneous dynamics. When the material is cooled from the melt state, the viscosity increases dramatically at the glass transition temperature, which is due to the percolation of small domains of slow dynamics within the system. The population of slow domains is controlled by the sample temperature, and the number of slow domains increases upon cooling. Once the network of slow domains is established, the glass transition occurs. According to Long and Lequeux, the slow domains percolate at a lower temperature in the case of quasi 2-dimensional free-standing thin films compared to a three-dimensional bulk system, and leads to a lower T_g in thin films.

The effects and understanding of confinement remain a challenge for the scientific community. In the present study, the confinement effects on T_g are seen in a nanoporous material. In a recent study, confinement effects on T_g were also observed in polymer nanocomposites. Bansal et al. [26] showed that a correlation between the T_gs of polymer nanocomposites and polymer thin films exists and that average particle-to-particle distances could be used to compare thin films and nanocomposite systems. A similar correlation should also exist for the PEI systems investigated in the present study. The nanopores provide a free surface similar to that observed in free-standing thin films. In addition, the thickness of the thin films should correlate with the pore-to-pore (surface-to-surface) distances. Therefore, the nearest neighbor distances with respect to pore volume fraction were calculated from the Monte Carlo simulations. The pores were randomly dispersed in the polymer matrix and the pore size distribution followed the lognormal distribution obtained from SEM measurements. Keddie's equation (Eq. (4)) can then be applied to model the T_g data from nanoporous PEI samples by substituting the film thickness with an appropriate pore-to-pore (surface-to-surface) distance. Since it is not obvious what pore-to-pore distance would be appropriate, various averages of the nearest neighbor distances were calculated (see Fig. 3 for nearest neighbor pore-to-pore distance distributions): arithmetic average, second moment average, and harmonic average. These are defined as follows:

Arithmetic average:

$$\overline{h} = \frac{\sum_{i=1}^{N} h_i}{N} \tag{6}$$

Second moment average:

$$\overline{\overline{h}} = \frac{\sum_{i=1}^{N} h_i^2}{\sum_{i=1}^{N} h_i} \tag{7}$$

Harmonic average:

$$h^* = \frac{N}{\sum_{i=1}^{N} \frac{1}{h_i}} \tag{8}$$

where h_i is the nearest pore-to-pore distance, and N is the number of nearest pore-to-pore distances calculated. Duplicate nearest neighbor distances were removed.

Fig. 7 shows the T_g data for nanoporous PEI as a function of the average pore-to-pore distances. The thin film data are represented by the solid line that shows the best fit curve obtained using Keddie's model (with $A = 3.38$ nm, $\delta = 1.61$). The arithmetic and harmonic averages obtained from the Monte Carlo simulations are positioned to the left of the thin film line, whereas the second moment averages are much closer to the thin film line, yielding at least a rough agreement between the two, although the shape (T_g vs. distance) is not exactly the same.

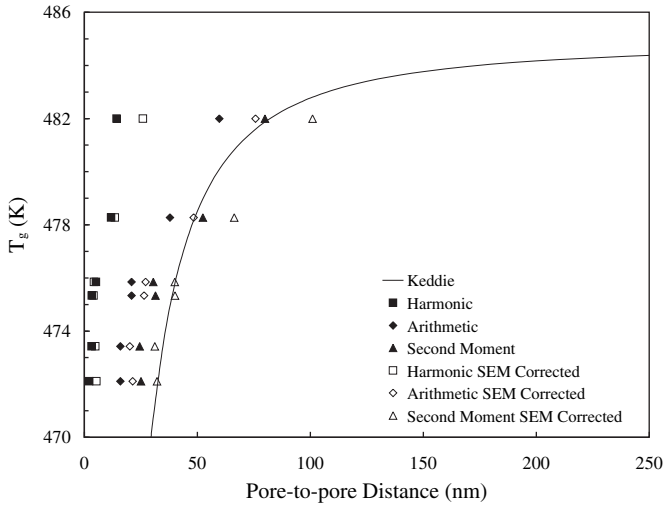

Fig. 7. Glass transition temperature as a function of various pore-to-pore (surface-to-surface) distance averages in the nanoporous PEI along with the Keddie equation fit to the PEI thin film data.

There are a couple of errors that might have arisen during the analysis. The Monte Carlo simulations used the lognormal pore size distribution function that was based on the pore size data obtained from the SEM measurements. SEM measurements sample an area, whereas the pores are three-dimensional. Therefore, SEM analysis provides only the "cross section" of a pore and the observed diameter does not represent the real diameter, unless the SEM cross section happens to slice the pore right at the center. The second possible error might have been caused by the Monte Carlo simulations. In the simulations, overlapping of pores were strictly forbidden, but it is possible that if two pores are too close, they would coalesce to form one larger pore. The effects of these two errors on the nearest neighbor distances will be discussed next.

The pore size data were obtained from the SEM analysis of the cross sectional areas of the samples. Unless the SEM surface intersects the pore at its center, the observed pore size is less than the real diameter of the pore. It is thus obvious that the pore size data collected through SEM analysis underestimates the real pore sizes. If in fact pores are larger than observed during SEM image analysis, there will be a smaller number of pores at a given pore volume fraction and the pore-to-pore distances would increase. This should shift the nanoporous T_g data shown in Fig. 7 to the right.

In order to calculate the error arising from the SEM analysis, it is assumed that the centers of the pores are uniformly distributed in the direction perpendicular to the SEM surface (along the z-axis). This assumption is correct and the error from this assumption can be minimized if the number of pores in the sample is high enough. In addition, the probability of the SEM image surface intersecting a pore, whose center is at $z = 0$, between $z = -R$ and $z = +R$ (R is the real radius of the pore), does not depend on the pore size (the SEM image surface can cut through the pore at any point along the z-axis with equal probability). Then, the average value of the ratio of the pore radius derived from the SEM analysis (r) to the actual pore radius (R) is given as follows:

$$\left(\frac{r}{R}\right)_{ave} = \frac{\int_{-1}^{+1} \sqrt{1-\left(\frac{z}{R}\right)^2} \cdot d\left(\frac{z}{R}\right)}{\int_{-1}^{+1} d\left(\frac{z}{R}\right)}, \tag{9}$$

where z is the location of the SEM surface along the z-axis. The analytical solution to Eq. (9) is given by the hypergeometric function, which gives $r/R = 0.785398$. Therefore, the SEM analysis of the nanoporous samples underestimates the real size of the pores by approximately 21.5%. This, of course, is the maximum error that could have arisen in our calculations. The solution to this error is very easy: during the Monte Carlo simulation, each pore can be divided by the r/R value given above to correctly account for the real size of the pore (R) rather than the observed pore size (r) during SEM image analysis. The results of this correction are also shown in Fig. 7 along with the uncorrected data. As expected, all average pore-to-pore distances increased and resulted in the shifting of the nanoporous data to the right (larger distances).

Also, stated before, the overlapping of pores was strictly prohibited during the initial Monte Carlo simulations. In order to investigate the effects of pore overlaps, we performed additional Monte Carlo simulations where random pore overlaps were allowed. If two (or more) pores overlapped, then these pores were considered as one pore with a volume equal to the sum of the overlapping pore volumes. This is a natural extension of the coalescence of pores during nucleation and growth in real systems. In real systems, if two (or more) pores overlapped during growth, the internal pressure within the growing pores would quickly stabilize (a common pressure would be reached), and initially what were separate pores would become one and grow as a single pore. When pore overlaps were allowed, the location of the new unified pore was calculated according to the volume average of the (initial) individual pores. The effect of allowing overlaps should thus increase the nearest neighbor distances because there would be fewer pores when overlapping pores are considered as one pore. The magnitude of this effect depends on the pore volume fraction, since the probability of pores overlapping with one another increases with the number of pores present. The effect of pore overlaps was very low at low pore volume fractions; less than 5% change in the nearest neighbor distances were observed. At high pore volume fractions, the effect was stronger; up to 50% increase in the nearest neighbor distances was observed.

If both the SEM and the overlap corrections are performed at the same time as they should be, all average nearest neighbor distances increase. This combined effect on the T_g vs. interpore spacing data is shown in Fig. 8, and indicates that the arithmetic average of the nearest neighbor distances best represents the nanoporous T_g data. This finding contradicts the observation of Bansal et al. [26], where the harmonic average nearest neighbor distance was found to best describe their nanocomposite data.

Based on these observations, an analogy between the nanoporous PEI and the PEI thin films can be proposed through the arithmetic average of the nearest neighbor pore-to-pore distances for the nanoporous PEI system. In both systems, the effects of confinement on the glass transition temperature were represented by the Keddie equation. Due to the localization of polymer chain ends, the free volume at the free-surface-like interface region increases, which enables the polymer chains to exhibit higher mobility than those in the bulk region. According to the percolation mechanism proposed by Long and Lequeux [21], the high mobility interface region contributes to disrupt the percolation of the slow domains when the system is cooled from the polymer melt. In confined systems, such as thin films and nanoporous systems, the interface regions are sufficiently close together, and the percolation of the slow domains is affected by these high mobility interface regions, which leads the glass transition to occur at a lower temperature compared to the bulk polymer. The percolation theory thus provides a mechanism to explain how the interface regions affect the T_g in confined systems. In addition, it also suggests a theoretical explanation for the Keddie equation, which was found

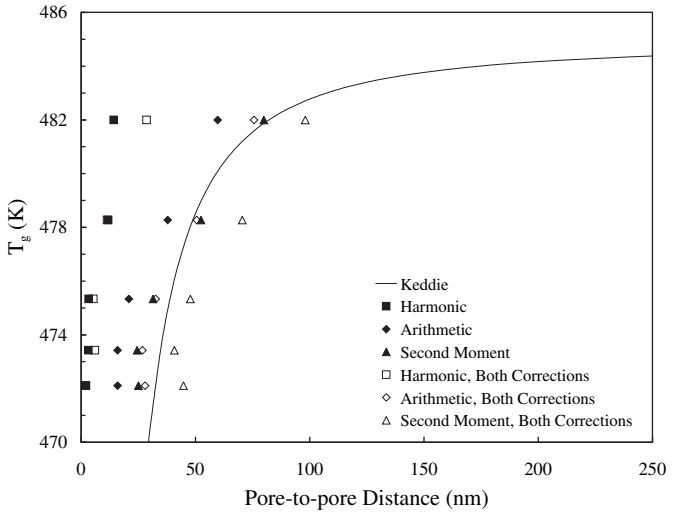

Fig. 8. Glass transition temperature as a function of various pore-to-pore (surface-to-surface) distance averages in the nanoporous PEI (closed symbols) along with the Keddie equation fit to the PEI thin film data. The effect of SEM pore size correction on the nanoporous T_g data is also presented (open symbols).

to fit the experimental observations in both PEI thin films and nanoporous PEI.

As a final point, we draw attention to the fact that two different nearest neighbor distance averages have now been shown to describe the effects of confinement: the harmonic average in the nanocomposite system by Bansal et al. [26] and the arithmetic average in the nanoporous system of the present study. The errors in our study have been considered, and hence corrections were performed to yield an accurate result. On the other hand, the interactions at a nanoparticle–polymer interface are more complicated than those at a free interface; hence, there does not need to be a direct correlation between the two systems. Although our analysis indicates that the arithmetic average best explains the nanoporous data, further research needs to be performed to assess the effects of confinement, and to verify if a common average length scale can explain the confinement effects due to both nanoparticles or nanopores, or if there is another reason for the apparent discrepancy such as the nature of the interactions at the interface.

5. Conclusions

A decrease in the glass transition temperature (T_g) from its bulk value was observed in both nanoporous polyetherimide (PEI) and PEI thin film systems. The deviation of T_g in confined systems is due to the effects of the interface regions. In particular, for a free-standing interface, the polymer chains have higher mobility in the interface region than in the bulk. These high mobility interface regions disrupt the percolation of slow domains in the system, leading to a decreased glass transition temperature, which provides further evidence for the percolation theory of the glass transition in polymers. Based on the present T_g study, an analogy between the nanoporous PEI and PEI thin films was observed. In the nanoporous polymers, the arithmetic average nearest neighbor pore-to-pore (surface-to-surface) distance corresponds to the film thickness in the polymer thin films. The relationship between T_g and pore-to-pore distance can be quantitatively described by the Keddie equation. When the high mobility interface regions in the system are sufficiently close together, the excess mobility in the interface region alters the dynamics further into the bulk region, which induces the confinement effects on T_g.

Acknowledgements

Financial support from IBM, the Nanoscale Science and Engineering Initiative of the National Science Foundation under NSF Award Number DMR-0117792 and CMMI-0500324 is gratefully acknowledged. Suggestions by Linda L. Schadler and Sanat K. Kumar are gratefully acknowledged.

References

[1] Jones RAL, Richards RW. Polymers at surfaces and interfaces. Cambridge: Cambridge University; 1999.
[2] Adams G, Gibbs J. J Chem Phys 1965;43:139.
[3] Ash BJ, Siegel RW, Schadler LS. J Polym Sci Part B Polym Phys 2004;42:4371.
[4] Schönhals A, Goering H, Schick Ch. J Non-Crystalline Solids 2002;305:140.
[5] Mattsson J, Forrest JA, Borjesson L. Phys Rev E 2000;62:5187.
[6] Keddie JL, Jones RAL, Cory RA. Europhys Lett 1994;27:59.
[7] Keddie JL, Jones RA, Cory RA. Faraday Discuss 1994;98:219.
[8] DeMaggio GB, Frieze WE, Gidley DW, Zhu M, Hristov HA, Yee AF. Phys Rev Lett 1997;78:1524.
[9] Fryer DS, Peters RD, Kim EJ, Tomaszewski JE, White CC, Wu WL. Macromolecules 2001;34:5627.
[10] Forrest JA, Dalnoki-Veress K, Dutcher JR. Phys Rev E 1997;56:5705.
[11] Forrest JA, Mattsson J. Phys Rev E 2000;61:R53.
[12] Ellison CJ, Torkelson JM. Nat Mater 2003;2:695.
[13] Jean YC, Zhang R, Cao H, Yuan JP, Huang CM, Nielsen B, et al. Phys Rev B 1997;56:R8459.
[14] Bliznyuk VN, Assender HE, Briggs GAD. Macromolecules 2002;35:6613.
[15] Sillis S, Overney RM. J Chem Phys 2004;120:5334.
[16] Jang JH, Ozisik R, Mattice WL. Macromolecules 2000;33:7663.
[17] Mayes AM. Macromolecules 1994;27:3114.
[18] von Meerwall E, Beckman S, Jiang J, Mattice WL. J Chem Phys 1998;108:4299.
[19] de Gennes PG. Eur Phys J E 2000;2:201.
[20] Dalnoki-Veress K, Forrest JA, de Gennes PG, Dutcher JR. J Phys IV France 2000;10:7–211.
[21] Long D, Lequeux F. Eur Phys J E 2001;4:371.
[22] De Lorenzo ML, Errico ME, Avella M. J Mater Sci 2002;37:2351.
[23] Pham JQ, Mitchell CA, Bahr JL, Tour JM, Krishanamoorti R, Green PE. J Polym Sci PartB Polym Phys 2003;41:3339.
[24] Ash BJ, Schadler LS, Siegel RW. Mater Lett 2002;55:83.
[25] Bansal A. Thermomechanical properties of polymer nanocomposites: exploring a unified relationship with planar polymer films. Troy: Rensselaer Polytechnic Institute; 2004.
[26] Bansal A, Yang H, Li C, Cho K, Benicewicz BC, Kumar SK, et al. Nat Mater 2005;4:693.
[27] Liu T, Ozisik R, Siegel RW. Thin Solid Films 2007;515:2965.
[28] NIST/SEMATECH e-Handbook of Statistical Methods, http://www.itl.nist.gov/div898/handbook; 2004.
[29] Sakai K, Ozawa K, Mimura R, Ohashi H. J Membr Sci 1987;32:3.
[30] Lusti HR, Gusev AA, Guseva O. Model Simul Mater Sci Eng 2004;12:1201.
[31] Paul DR, Newman S. Polymer blends. New York: Academic; 1978.
[32] Li X, Han Y, An L. Polymer 2003;44:8155.
[33] Moons E. J Phys Condens Matter 2002;14:12235.
[34] Mooney CZ. Monte Carlo simulation. London: Sage; 1997.